32. M. Salomon, *This Journal*, **117**, 325 (1970).
33. V. A. Pleskov, *Usp. Khim.*, **16**, 254 (1947).
34. V. A. Pleskov, *Zh. Fiz. Khim.*, **22**, 351 (1948); *Chem. Abstr.*, **42**, 6249.
35. H. Lund, *Acta Chem. Scand.*, **11**, 491 (1957).
36. T. Pavlopoulos and H. Strehlow, *Z. Physik. Chem. (Frankfurt)* **2**, 89 (1954).
37. W. M. Latimer, "Oxidation Potentials," Prentice-Hall, Englewood Cliffs, N. J. (1952).
38. K. K. Kundu, A. K. Rakshit, and M. N. Das, *Electrochim. Acta*, **17**, 1921 (1972).

Electrogenerated Chemiluminescence

XXIII. On the Operation and Lifetime of ECL Devices

Daniel Laser and Allen J. Bard*

Department of Chemistry, The University of Texas at Austin, Austin, Texas 78712

ABSTRACT

Factors affecting the lifetime of ECL devices, including decomposition of starting materials, formation of side products which react with radical ions or quench excited states, and filming of the electrodes are discussed. The mode of operation of the ECL device is shown to be important in determining its behavior and lifetime; operation of (*i*) three-electrode pulsed potentiostatic, (*ii*) two-electrode pulsed voltage, (*iii*) two-electrode pulsed constant current, and (*iv*) thin-layer cells is discussed and illustrated, in studies of the $Ru(bip)_3^{2+}$ system in acetonitrile and the rubrene system in benzonitrile.

Electrogenerated chemiluminescence (ECL) involves the production of excited state species and ultimately light from the reaction of electrogenerated oxidants and reductants (1-7). Since several ECL systems are capable of producing fairly bright light at reasonable electrical efficiencies, several applications of practical devices based on the ECL phenomenon, *e.g.*, lasers, display devices, image convertors, etc. (8-12), have been suggested. For these devices to be practical, however, good lifetimes of the systems are required. In principle an ideal ECL system involving stable electrogenerated reactants (*e.g.*, a radical anion, $A^{\cdot -}$, and radical cation, $D^{\cdot +}$) should show a very long lifetime, since the ECL cycle (*e.g.*, Eq. [1]-[4]) involve no net chemical change in the system. In fact most ECL systems show a decay in emission with

$$A + e \rightarrow A^{\cdot -} \quad [1]$$

$$D - e \rightarrow D^{\cdot +} \quad [2]$$

$$A^{\cdot -} + D^{\cdot +} \rightarrow A^* + D \quad [3]$$

$$A^* \rightarrow A + h\nu \quad [4]$$

time (minutes to hundreds of hours) under continuous electrical excitation. The rate of this decay depends on the nature and purity of the ECL system as well as the design of the ECL cell and the form of the electrical excitation. It is the purpose of this paper to discuss the factors affecting the lifetime of ECL cells and give examples of the behavior of these devices under different experimental conditions.

Experimental

Purification of the solvents, acetonitrile (ACN) and benzonitrile (BZN), the supporting electrolyte, tetra-*n*-butylammonium perchlorate (TBAP), and the reactants followed previous practice (7, 11). All experiments were conducted in a Vacuum Atmospheres (Los Angeles, California) Glove Box equipped with a Model MO 40-1 Dri-Train.

The macro-cell had a solution volume of 30 mliters with an optically flat Pyrex glass window. The working electrode was a polished platinum disk (0.25 cm^2) sealed flush into soft glass and aligned parallel to, and about 1 cm away from, the window. The large auxiliary electrode was a platinum foil (*ca.* 5 × 2 cm) surrounding the working electrode and immersed directly in the test solution. The reference electrode was a silver wire immersed in $10^{-2}M$ $AgNO_3$ in ACN, contained in a 6 mm glass tube closed at the bottom by a plug of porous Vycor (Corning Type 7930 "thirsty glass"), which was held to the glass tube by a piece of shrinkable Teflon tubing. For experiments with working and auxiliary electrodes of equal size, two matched Pt wires were employed.

The thin-layer ECL cells were constructed with two pieces of transparent Cu-doped SnO_2 glass (Corning), *ca.* 20 ohm/square, spaced apart by a thin Teflon spacer, and clamped by spring clamps. The active electrode area in these cells was *ca.* 0.5 cm^2.

All electrochemical measurements were made with a Princeton Applied Research Corporation Model 176 instrument, with a Wavetek Model 114 function generator, a Mosley Model 7005A XY recorder, and a Tektronix Model 564 dual beam oscilloscope. Relative light intensities were measured with a Centralab Semiconductor solar cell attached to the ECL cell window.

Results and Discussion

Failure modes.—There are several modes by which an ECL system will undergo changes which will ultimately cause a substantial decrease in light emission. These are:

1. Loss of the electroactive substances A and/or D, leading to a decrease in the concentration of the reacting ions $A^{\cdot -}$ and $D^{\cdot +}$, and thus of the emitting species. This frequently occurs when the radical ion species $A^{\cdot -}$ or $D^{\cdot +}$ decay by reaction with solvent or impurities; in this case the rate of decay of intensity is related to the kinetics of the decomposition reaction (13, 14). In several systems, *e.g.*, A = D = rubrene (in BZN or DMF), A = D = *tris*-bipyridylruthenium(II) (in ACN), A = 9,10-diphenylanthracene (DPA), D = thianthrene (in ACN), the radical ion species are very stable, and ECL

* Electrochemical Society Active Member.

Key words: electrochemiluminescence, nonaqueous solvents, thin-layer electrochemistry, radical ions, cyclic voltammetry.

systems which have failed show no or only a very small change in the A and D concentrations as determined by cyclic voltammetry or spectroscopy before and after the ECL experiment. However if the electrode potential is not closely controlled and is allowed to move to regions where later waves (*e.g.*, production of A^{2-} or D^{2+}) or electrolysis of solvent or supporting electrolyte occurs, then loss of A and D can be significant. This occurs because of instability of the dianion and dications of most organic species employed in ECL. This can happen even in three-electrode potentiostatic experiments if the reference electrode potential drifts during the lifetime test or if the system goes into large oscillations during adjustment of the positive feedback *iR*-compensation circuit. When this occurs the solution often turns a brownish color and it cannot be restored to a light-emitting condition.

2. Production of small amounts of side products from slow reactions of $A^{\cdot -}$ or $D^{\cdot +}$ with other system components or impurities; these side products can react with $A^{\cdot -}$ or $D^{\cdot +}$ decreasing their life or they may act as quenchers of the excited states. These decomposition reactions could involve reactions of A^{2-} (formed on disproportionation of $A^{\cdot -}$) or D^{2+} (formed on disproportionation of $D^{\cdot +}$). Although the equilibrium constants for these disproportionation reactions are small (*e.g.*, 10^{-8} for a *ca.* 0.5V separation between E° values of radical ion and doubly charged ion half-reaction), the dianions and dications are usually very reactive species; this disproportionation decay of radical ions, in connection with much faster reactions, however, has been discussed extensively (15-17). A useful estimate of the maximum rate of buildup of side-product (or rate of loss of reactant) can be derived as follows: Assuming that the electrolysis of the reacting component (*e.g.*, A) is diffusion controlled, the moles of species A electrolyzed per pulse is

$$\text{moles electrolyzed per pulse} = \int_0^{t_f} i\,dt/\mathbf{F} = 2AC\,(Dt_f/\pi)^{1/2} \quad [5]$$

where C and D are the concentration and diffusion coefficient of A, t_f is the pulse length, and A the electrode area. If $A^{\cdot -}$ decomposes by a first-order or a pseudo-first-order reaction with a rate constant, k, the fraction of $A^{\cdot -}$ converted to product, Q, is $1 - e^{-kt_f}$. Thus the maximum number of moles of Q produced per pulse is

$$\text{moles } Q \text{ produced per pulse} = 2(1 - e^{-kt_f})AC(Dt_f/\pi)^{1/2} \quad [6]$$

The concentration of Q produced in the total solution volume, V, after N pulses is

$$[Q] = 2(1 - e^{-kt_f})C\,N(A/V)\,(Dt_f/\pi)^{1/2} \quad [7]$$

The total system lifetime, T, is $2Nt_f$. Moreover, in any practical system kt_f is small, so that $1 - \exp(-kt_f)$ is essentially kt_f. With these substitutions the lifetime can be approximated by

$$T = ([Q]/C)\,(V/A)\,(\pi/Dt_f)^{1/2}/k \quad [8]$$

The time required to build up a significant concentration of side product for a given k, depends on the pulse length and V/A ratio. For example, for the typical values, $D = 5 \times 10^{-6}$ cm^2/sec and $t_f = 0.01$ sec, and assuming the device lifetime is attained when the impurity level builds up to 1% of starting substance ($[Q]/C = 0.01$), the lifetime expression is

$$T(\text{hr}) \simeq 0.02\,(V/A)\,(\text{cm})/k\,(\text{sec}^{-1}) \quad [9]$$

Thus a 1000 hr lifetime requires $k < 2 \times 10^{-3}$ sec^{-1} for a V/A ratio of 100 cm, characteristic of a large scale cell, while a $k < 2 \times 10^{-7}$ sec^{-1} is required for a V/A ratio of 10^{-2} cm, typical of a thin-layer cell.

The decreased lifetime of the radical ion species is signaled by decreased reversal currents in cyclic voltammetry over those originally observed. These side products can also behave as quenchers of the generated excited states. The radiative lifetime of singlet states is short (about 10^{-8} sec) so that small concentrations of generated quenchers should not be of importance in ECL systems where singlet excited states are produced directly on reaction of $A^{\cdot -}$ and D^{+} [*i.e.*, S-route systems, *e.g.*, DPA(−)/DPA(+) in DMF]. However triplet states have longer radiative lifetimes (10^{-3} to several seconds) and can be quenched by low concentrations of side products. Thus systems which involve direct formation of triplets followed by triplet-triplet annihilation to produce emitting singlets [T-route systems, *e.g.*, rubrene(−)/rubrene(+) in DMF and many energy deficient mixed systems] may be susceptible to this decay mode. In certain special cases photochemical-type reactions of the excited state species (rearrangements, cycloadditions, etc.) could also occur.

The applied excitation signal also affects this decay mode. The assumption has been made that the anodic and cathodic coulombs were equal, so that no excess of either $A^{\cdot -}$ or $D^{\cdot +}$ is produced over long, repeated pulsing. However this condition is only obtained by careful control and appropriate relative electrode areas. In the absence of this condition one of the reactants builds up in the bulk solution and can show more extensive decomposition to side products.

3. Production of side products from the electrolysis of impurities in the solvent, supporting electrolyte, or radical ion precursors, which can react with $A^{\cdot -}$ and/or D^{+} or quench the excited states. For example traces of water, which are difficult to remove from solvents such as DMF and ACN, could be oxidized on anodic pulses to oxygen, which in turn could be reduced to $O_2^{\cdot -}$ on cathodic pulses. Electrogenerated $O_2^{\cdot -}$ has been shown to react as a nucleophile and as a base (18). In the process free radicals such as $HO_2\cdot$ and $HO\cdot$ are produced, which may initiate chain reaction decomposition of system components. Since 2 ppm water represents 0.1 mM water, or 1-10% of the A and D species, very high purities of system components are required. If electrolysis of the solvent or supporting electrolyte occurs, either because of lack of control of the applied signal or because the radical ion generation processes occur on the foot of background discharge, deleterious substances can also be generated. For example, it is known that the light level of the DPA(−)/DPA(+) in the DMF system decreases sharply when the potential of the Pt generating electrode reaches those where cathodic background currents become appreciable (19).

4. Filming of the electrode by production of insoluble products (*e.g.*, polymers) from side reactions of the radical ions, or by electrolysis of impurities, solvent, or supporting electrolyte. These films can cause progressive blockage of the electrode or by buildup of a layer which can catalyze side reactions. When this form of decay is important, removing and polishing the electrode and returning it to the ECL system will at least partially restore the emission. This behavior was noticed upon generation of $DPA^{\cdot -}$ in ACN (19); other examples of filming are discussed below.

Electrical excitation of ECL.—The discussion of failure modes points to the importance of the mode of electrical excitation to long term stability. In general a desirable mode of excitation will (*a*) maintain the electrode potentials of both working and auxiliary electrodes in regions where only $A^{\cdot -}$ and $D^{\cdot +}$ can be produced; (*b*) be coulometrically symmetric, *i.e.*, have equal anodic and cathodic (faradaic) coulombs on alternate pulses; (*c*) maximize reaction between $A^{\cdot -}$

and D^+, *i.e.*, cause the direct oxidation of A^- and reduction of D^+ at the electrode to be minimal. For example the square wave potentiostatic mode causes very little loss of the radical ions by direct electrolysis, while appreciable losses occur with the sinusoidal or triangular wave potentiostatic or constant current modes.

Potentiostatic (three-electrode) pulsed mode.—This method is that employed in most recent experimental ECL studies and has been treated theoretically (13, 14, 20). With regard to operation of a long-duration cell the design of the reference and auxiliary electrodes becomes important. The reference electrodes frequently employed in ECL are silver or platinum wire quasi-reference electrodes which show reasonable stability over experiments of a few hours duration but which show much too large drifts in potential with continuous pulsing over long time periods to be reliable. Other, more poised, reference electrodes, like the aqueous saturated calomel electrode (SCE) can leak undesirable amounts of water or alkali metal ion into the ECL solution on prolonged immersion, even when separated with double sintered-disk salt bridges. We have found that the Ag/Ag^+ (ACN) contained in a porous Vycor tube, as described in the Experimental section, maintained a reproducible and constant potential, and showed no detectable leakage of Ag^+ into the main body of solution after many tens of hours of use. The auxiliary electrode design is also of importance, since uncontrolled electrochemical processes occur there and these may lead to solution contamination. The usual electrochemical technique of isolating the auxiliary electrode in a separate chamber separated from the working electrode chamber by sintered glass disks, salt bridges, etc., is not desirable in ECL since this greatly increases the power necessary to drive the cell, and may prevent potentiostatic control of the working electrode in the early stages of pulse reversal when large currents flow. An auxiliary electrode which is somewhat larger than the working electrode and immersed directly into the ECL solution compartment in a geometry where the current density across its surface is fairly uniform can be employed. The current density at its surface will be smaller than that at the working electrode, and hence it will attain less negative and less positive potentials (with respect to the adjacent solution) than those of the working electrode. Certainly a small auxiliary electrode is to be avoided, since it will be forced to more negative and positive potentials causing undesired electrode reactions to supply the current required for potentiostatic control of the working electrode. The role of the auxiliary electrode is illustrated in a discussion of two-electrode cells in the next section.

To illustrate the necessity of potential control and the behavior of an ECL system under continuous long-term pulsing we consider the *tris*-bipyridylruthenium(II) ($Ru(bip)_3^{2+}$) system in ACN. The electrochemistry and ECL of this system have been described (21, 22). Briefly, $Ru(bip)_3^{2+}$ undergoes three reversible reduction steps (to the +1, 0, and −1 species) and a reversible oxidation (to the +3 species) in dry, deoxygenated ACN (Fig. 1). Controlled potential coulometry experiments have demonstrated that the +3 species is very stable, but that the +1 species, although apparently stable on the cyclic voltammetric time scale, undergoes a very slow decomposition reaction (22). ECL results from reaction of the +3 species with either the +1, 0, or −1 generated on the cathodic cycle. The application of alternate potential steps between +1.200 and −1.900V *vs.* Ag/Ag^+ with 95% *iR* compensation, *i.e.*, from oxidation to second reduction wave, with a frequency of 100 Hz (*i.e.*, t_f = 5 msec) in a cell with $V = 20$ cm^3 and $A = 0.25$ cm^2 produced intense ECL with a half-life, $T_{1/2}$, (the time for the ECL intensity to decrease to one-half its initial value), of about 5 hr.

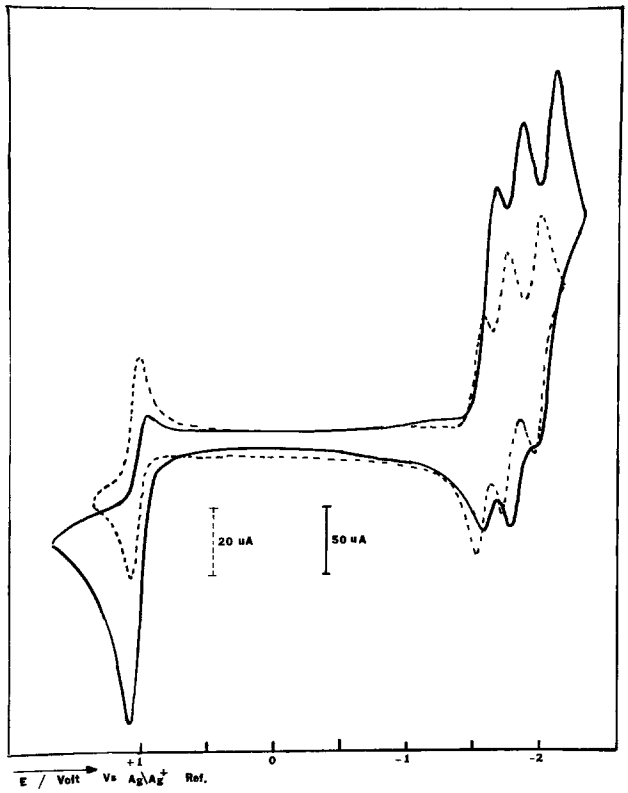

Fig. 1. Cyclic voltammetry of 0.6 mM $Ru(bip)_3(ClO_4)_2$/0.1M TBAP/ACN solution at Pt electrode with a scan rate of 100 mV/sec. - - - -, Original solution; ———, the same solution after 5 hr of ECL production by pulsing between +1.20 and −1.90V at 100 Hz after which no further ECL emission is observed.

The cyclic voltammogram at this time taken at the same working electrode in the ECL cell is noticeably different than the original one (Fig. 1). The height of the reduction peaks ($+2 \rightarrow +1$, $+1 \rightarrow 0$, $0 \rightarrow -1$) depend on the positive potential the electrode has attained during the anodic scan; they are larger (and anomalous) when the anodic scan includes the +2/+3 wave than when the scan stops at the foot of this wave. Similarly the +2/+3 wave is anomalous when the cathodic scan includes the +2/+1 wave. This behavior is evidence of surface changes at the electrode causing changes in electrochemical reaction. Furthermore a yellow-brown precipitate covers the electrode surface. If the electrode is removed from the ECL cell in an inert atmosphere box, polished with 0.03μ alumina and replaced, both the original cyclic voltammetric behavior and the original ECL intensity is restored.

The nature of the interfering precipitate was elucidated by some experiments at the RRDE. As shown previously (22) when the disk potential is held at the second reduction wave (production of $Ru(bip)_3^{\circ}$) and the ring potential held at the foot of the first reduction (corresponding to oxidation $0 \rightarrow +2$), the disk current, after a short time of constancy equal to twice the current of the first reduction wave, begins to increase with time (up to a one order of magnitude increase) without a corresponding increase in the ring current. This lack of increase in the ring current demonstrates that the increasing disk current cannot be attributed to formation of soluble $Ru(bip)_3^{\circ}$. If the disk potential is scanned back toward more positive potentials a large oxidation disk current peak is observed at potentials corresponding to the $+1 \rightarrow +2$ wave. A similar large oxidation current peak is seen at the ring at this time (E_R = 0.0V). These results can be explained by the formation of a deposit on the disk electrode. This deposit catalyzes the reduction of solvent or electrolyte (giving rise to the enhanced disk current) and is oxidatively stripped off during the positive potential

sweep. The nature of the deposit has not been established. It could be some form of $Ru(bip)_3^{\circ}$ itself or Ru-metal formed by its decomposition. Attempts to reproduce this effect on a stationary Pt electrode by electrodeposition of finally divided Ru-metal were unsuccessful. A deposit of a zero-valent Ru-species would explain the stripping experiment, if the disk oxidation peak represented the oxidation of this deposit to the +1 species while the ring current represented the further oxidation of $+1 \rightarrow +2$. An alternate explanation would require falling away of some of the zero-valent species during the oxidation scan producing +1 species (upon reaction with +2 in the gap region) which is oxidized at the ring. Thus for the long duration ECL with the $Ru(bip)_3^{+2}$ system the second reduction wave must be avoided; pulsing to the second reduction wave is also undesirable, because of lack of coulombic symmetry and the consequent slow buildup of reduced species in the bulk solution. Since the first and second reduction waves are separated by only about 200 mV, close potential control (better than ±50 mV) is required, with the negative potential limit adjusted between $E_{p/2}$ and E_p of the first reduction wave. The positive potential limit was at or beyond that peak for the oxidation to the +3 species. Under these conditions, with pulsing between −1.650 and +1.100V at 100 Hz for a 2.5 mM $Ru(bip)_3^{2+}$, 0.1*M* TBAP solution in ACN, the ECL emission increased slightly from its initial value and maintained this level for 50 hr. The intensity-time behavior in this system is shown in Fig. 2; the experiment was terminated at 112 hr. Cyclic voltammetry after this period shows no change in $Ru(bip)_3^{2+}$ concentration, but evidence for production of a small amount of an unidentified electroactive species is found (Fig. 3).

Voltage (two-electrode) pulsed mode.—Practical ECL devices will probably be based on two-electrode systems. The way in which the potentials of the working electrode and the counterelectrode vary during pulsing with a low impedance function generator depend on the cell geometry and relative electrode areas. In this mode the technique of applying a symmetrical square wave to the cell and increasing the voltage until maximum emission is observed or alternatively applying a signal of $\pm\Delta E_p$ (the peak potential separation) can result in overdriving the cell and degraded device life.

Before the system is perturbed both electrodes are at their open-circuit or rest potentials, which will be essentially identical, if both electrodes are composed of

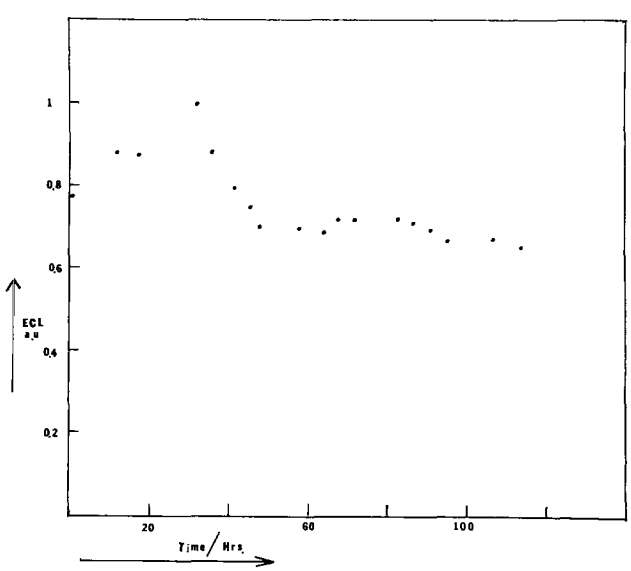

Fig. 2. ECL intensity vs. time behavior for a 2.5 mM $Ru(bip)_3(ClO_4)_2$/0.1M TBAP/ACN solution with pulsing between +1.200 and −1.650V vs. Ag/Ag^+ (ACN) electrode at 100 Hz.

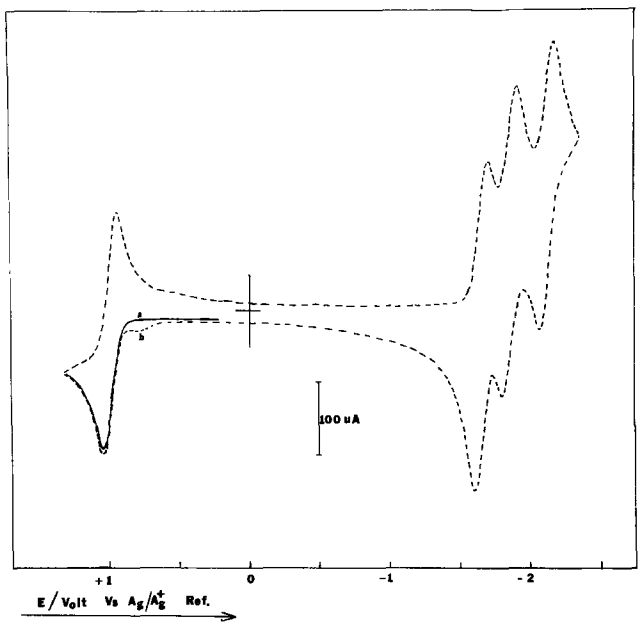

Fig. 3. Cyclic voltammetry of the system of Fig. 2 at a scan rate of 100 mV/sec. (a) Original solution; (b) after 120 hr of ECL production.

the same material and have been subjected to similar pretreatments; this rest potential will generally be somewhere between the $A/A^{-\cdot}$ and $D/D^{+\cdot}$ half-reaction potentials. When the voltage step, *V*, is applied between the working and counterelectrodes the potentials of the electrodes move in opposite directions such that their difference plus the solution *iR*-drop equals *V*, with the current in one electrode being equal in magnitude and opposite in direction from that in the other. When the pulse is reversed the electrode potentials switch to new values which again satisfy the aforementioned conditions, but in general they do not simply interchange the potentials observed during the first pulse. Let us consider two possible cases when (*a*) the auxiliary electrode is much larger than the working electrode and (*b*) both electrodes are the same size and the rest potential lies about midway between the peaks.

In case (*a*) the current at the auxiliary electrode during the pulse will be largely (or even completely) nonfaradaic and will be consumed in charging the electrical double layer (dl) *i.e.*, most of the current will be consumed in moving the electrode potential of the auxiliary from its rest potential, but the potential of this electrode will not attain a value where a faradaic reaction can occur. The shift in the auxiliary electrode potential is thus inversely proportional to its dl capacity and hence its area; if the area is large enough (compared to the coulombs passed during the pulse), its potential will only shift very slightly from the rest potential. For the small area working electrode however, the electrode rapidly charges its dl and then carries out a faradaic oxidation or reduction. Under these conditions the small working electrode shifts by almost the total of the applied pulse, *V*. For example, if the working electrode moved immediately to the diffusion-limited plateau region, the faradaic current in the system would be governed by the Cottrell equation and the total coulombs passed during the pulse would be given by [5] plus the coulombs needed to charge the working electrode Q_{dlw}. The large auxiliary electrode, of area A_{aux}, will only shift by an amount ΔE_{aux}, given by

$$\Delta E_{aux} = \frac{2A_w\mathbf{F}(Dt_f)^{1/2}\pi^{-1/2} + Q_{dlw}}{A_{aux}C_{dl}} \qquad [10]$$

where C_{dl} is the dl capacity per unit area of the auxili-

ary electrode. For example, for $A_w/A_{aux} = 100$, concentrations in the mM range, and C_{dl} of 10 μf/cm^2, ΔE_{aux} will be about 100 mV for a 100 msec pulse. To illustrate this effect, we describe an ECL experiment with a solution of 2 mM rubrene and 0.1M TBAP in benzonitrile, with two platinum electrodes of ratio 80:1. An Ag/Ag$^+$ reference electrode was employed to monitor the potentials of both electrodes as a voltage pulse of $\pm$2.1V was applied across the Pt electrodes at a frequency of 10 Hz. The results, shown in Fig. 4, demonstrate that the large auxiliary electrode stays within $\pm$100 mV of its rest potential (+0.6V *vs.* reference electrode), while the small electrode moves $\pm$2V, from its rest potential to potential regions where secondary electrode reactions occur. (The slightly larger shift of the auxiliary electrode potential immediately after pulse reversal is caused by the large iR-drop at this time which is included mainly in the measured auxiliary electrode potential, because the reference electrode was located near the small working electrode). Thus, for this configuration, the large auxiliary electrode behaves as a practical reference electrode and the proper potential program can only be achieved by knowing the system rest potential and applying an unsymmetrical voltage program derived from the cyclic voltammetry of the system. If the rest potential does not lie exactly midway between the redox potentials for reduction and oxidation, an applied symmetrical (square) wave equal to one-half the peak separation either may not produce efficient ECL or may lead to "overpulsing" and shortened lifetime. Certainly a square wave of amplitude equal to the peak separation will lead to rapid system deterioration.

Case (*b*) involves two electrodes of the same size with the rest potential lying approximately midway between the peak potentials. In this case both electrodes will shift about the same amount in potential in opposite directions from the rest potential, *i.e.*, the applied potential is shared between the electrodes. This effect is illustrated in Fig. 5, where the conditions are the same as case (*a*) (Fig. 4), except that the electrodes are of equal size. Here both of the working electrodes shift by about $\pm$1V *vs.* the reference electrode for the $\pm$2.1V applied; the slight asymmetry in the shifts is caused by the rest potential not lying exactly midway between the peak potentials, but, in fact, lying about 50 mV toward E_{pa}. Thus the desired potential program for two equal size electrodes involves applied voltages essentially twice as large as for the very small-very large case, but both electrodes produce light. If the rest potential does not lie midway between the peaks, the general behavior will be the same, but the unequal extent of charging of the two electrodes will make behavior more complicated when the amount of nonfaradaic charge per pulse is appreciable.

For the general case of two electrodes of unequal, but not very disproportionate, size, the behavior will be intermediate to cases (*a*) and (*b*) above, and a carefully selected and controlled potential program is required; a symmetrical square wave will, in general, not be suitable.

Constant current pulsed mode.—A two-electrode mode in which alternate anodic and cathodic constant current pulses are applied has been suggested (23). This mode has the advantage of precise coulombic symmetry with simple control circuitry. However, the coulombic ECL efficiency is smaller in this mode and the applied current density, i_o, and pulse duration, t_f, must be maintained in a rather narrow range to obtain ECL yet prevent overdriving. The applied current again is distributed between dl charging and the faradaic process; in this case the rate of dl charging is controlled by i_o, with appreciable charging occurring before any faradaic process begins. Thus $i_o t_f$ must be larger than the

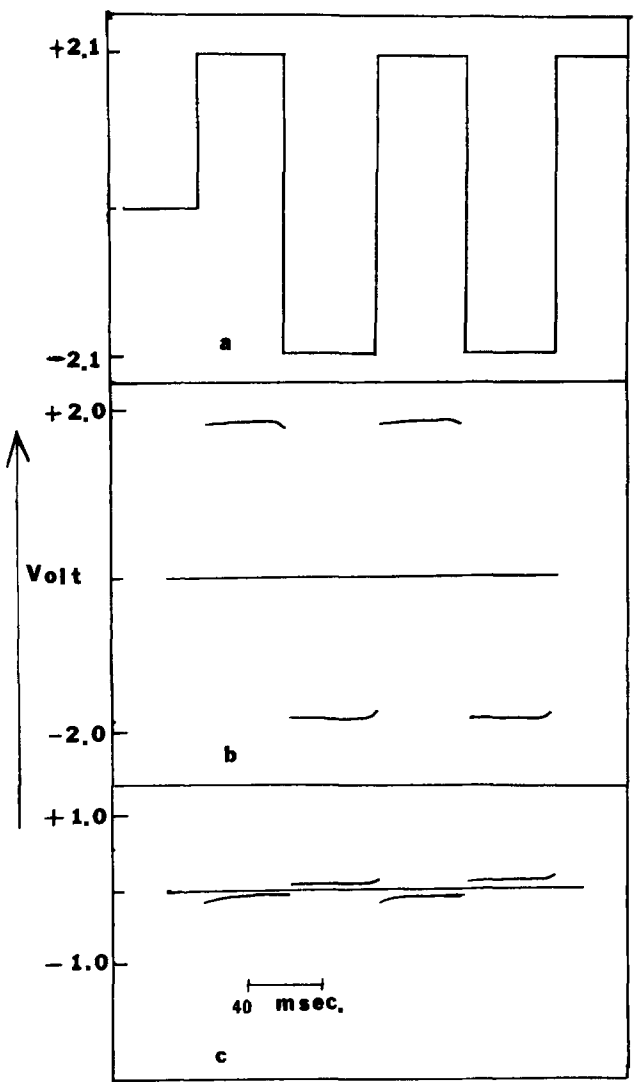

Fig. 4. Potentials of working and auxiliary electrodes (area ratio *ca.* 1:80) in the two-electrode voltage pulsed mode of operation. The solution was 2 mM rubrene/0.1M TBAP/BZN. (a) Applied voltage; (b) potential displacement of small electrode; (c) potential displacement of large electrode.

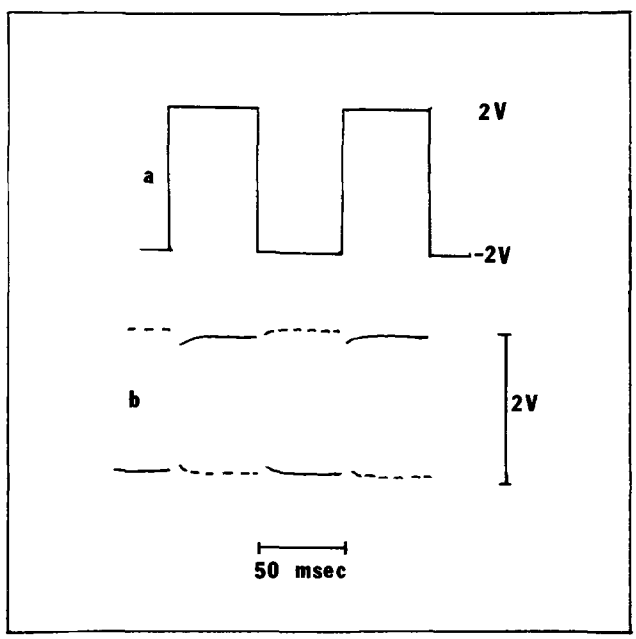

Fig. 5. Potentials of working and auxiliary electrodes (area ratio 1:1) in the two-electrode voltage pulsed mode. Solution as in Fig. 4. (a) Applied voltage; (b) potential displacement of electrodes.

number of coulombs required to charge the dl, approximately $C_{dl}\Delta E$ (*i.e.*, about 2×10^{-5} coulombs/cm^2 for 10 μf/cm^2 dl capacity and 2V step). However $i_o t_f^{1/2}$ must be maintained below $i_o\tau^{1/2}$, where τ, the chronopotentiometric transition time, is given by (24)

$$i_o\tau^{1/2} = \pi^{1/2}FnD^{1/2}C/2 = 85.5\ nD^{1/2}C\ (\text{mA-sec}^{1/2}) \quad [11]$$

if the electrode potential is to be maintained at values where secondary electrode reactions do not occur. Actually Eq. [11] pertains to a single constant current step; the transition time under constant pulsing conditions with continuous regeneration of parent will be close to this value. The useful working range of i_o and t_f in ECL based on these criteria is shown in Fig. 6, under the simplified assumption that dl charging is separable from the faradaic process.

With constant current ECL, upon reversal, the current first is consumed totally in reversing the process of the preceding pulse, without generation of a reacting species required for light emission. For example, if the first current pulse was cathodic and led to production of $A^{-\cdot}$ (Eq. [1]), then during the time period up to $(1/3)t_f$, the next anodic pulse would totally involve the oxidation of $A^{-\cdot}$ to A, as is usual for reversal chronopotentiometry (25). After this time the potential jumps in a positive direction, at a rate primarily determined by dl charging, to values where oxidation of D occurs (Eq. [3]). During this transition period oxidation of $A^{-\cdot}$ to A continues. However once $D^{+\cdot}$ production begins at the electrode, direct electrode oxidation of $A^{-\cdot}$ becomes negligible and ECL commences. The observed experimental behavior (Fig. 7) shows the delay in emission intensity on reversal, followed by a sharp increase, a maximum, and slow decay, in agreement with the results obtained by a digital simulation for this mode of operation.

The maximum steady-state ECL efficiency under these conditions, neglecting dl charging, is 0.62 that for the potential-step mode. The simulation results also predict an intensity proportional to the current, independent of cycling frequency. Moreover the total number of photons emitted per pulse is proportional to i_o at fixed frequency, is proportional to t_f at fixed i_o, and is inversely proportional to i_o at fixed $i_o t_f^{1/2}$. In practice,

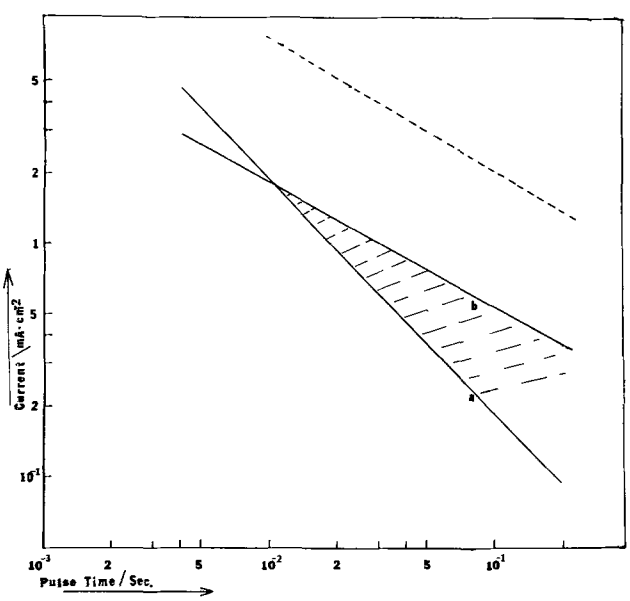

Fig. 6. Useful working region for pulsed constant current ECL. (a) Double layer charging limit, assuming $it_p = 20$ μcoulombs/cm^2; (b) upper (transition time) limit for $i\tau^{1/2} = 0.2$ mA · sec/cm^2 (*i.e.*, for $n = 1$, $D = 5 \times 10^{-6}$ cm^2/sec and $C = 1$ mM); - - - -, upper limit for *i* as in (b), except for $C = 2$ mM.

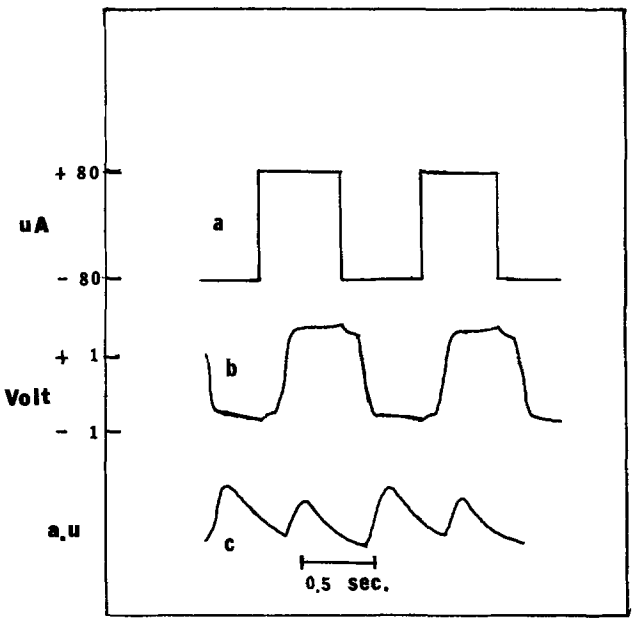

Fig. 7. Pulsed constant current ECL for a 2 mM rubrene/0.1M TBAP/BZN solution. (a) Applied current; (b) working electrode potential; (c) light intensity.

however, dl charging is not negligible, so that although the proportionality to i_o at fixed t_f is observed (Fig. 8A), the intensity is relatively smaller at higher frequencies because of the relatively greater importance of the nonfaradaic processes at small t_f values (Fig. 8B). Within the limitations of the method, however, this operation mode may be preferred to a controlled voltage mode for long lifetime operation.

Special controlled current modes which conserve the desirable features of constant current operation but overcome some of its problems, are also possible at the expense of greater driver complexity. For example a double pulse current mode, similar to that used in galvanostatic studies of fast electrode reactions (26) could be employed. This would involve a short, very large current pulse to charge the dl and, in ECL, also rapidly drive the electrode potential into the region where ECL begins, followed by a lower current of magnitude sufficient to maintain ECL (if the second

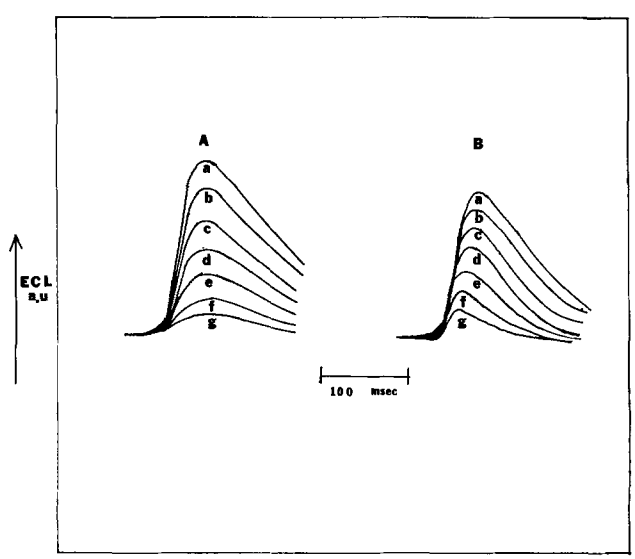

Fig. 8. Light intensity profiles in pulsed constant current ECL (conditions as in Fig. 7) with (a) pulsing at 1 Hz for currents of a-g 100, 90, 80, 70, 60, 50, 40 μA; (b) constant current of 100 μA for pulsing at 1, 1.2, 1.4, 1.6, 1.8, 2.0, 2.2 Hz, respectively.

current were too low the potential would drop back to the region where only reversal, *e.g.*, $A^{-\cdot} \rightarrow A$, occurred). This double pulse, constant current mode would require very careful adjustment and control to prevent overdriving, however.

Thin-layer cell, d-c mode.—Thin-layer ECL involves the use of two closely spaced electrodes (at least one of which is transparent) in which, during d-c electrolysis, the oxidized and reduced forms produced at the different electrodes diffuse (and migrate) together, near the middle of the interelectrode spacing, to annihilate, and produce light, and regenerate starting materials. The basic principles of thin-layer electrochemistry have been reviewed (27-29) and some thin-layer ECL experiments have been attempted (30-32). Thin-layer ECL has the advantage of producing a continuous and steady-state light with a low voltage d-c excitation. Only the rotating ring-disk electrode (RRDE) has been capable of producing true steady-state ECL previously (19). Moreover the close spacing minimizes the iR drop between the electrodes and the d-c operation eliminates charging current contributions, except during the initial switching on of the cell. However the very small cell volume places severe requirements on solution purity and reactant stability if long-life operation is to be attained.

The behavior of a thin-layer ECL cell follows that of the usual twin-electrode thin-layer cell (27-29), except that the concentration profiles of the electrogenerated reactants ($A^{-\cdot}$ and $D^{+\cdot}$) are such that, assuming equal diffusion coefficients and equal concentrations of A and D, both will have zero concentration in the middle of the cell at steady state. Thus, the limiting steady-state current will be

$$i_{ss}^{lim} = n\mathbf{F}ADC/0.5l \qquad [12]$$

where l is the interelectrode spacing (cavity thickness); the concentration profiles of $A^{-\cdot}$ and $D^{+\cdot}$ will be linear. The steady-state current-applied voltage behavior of the cell, assuming reversible electrode reactions, will be given by

$$\Delta V = \Delta E_{1/2} + \frac{2RT}{n\mathbf{F}} \ln\left(\frac{i_{ss}^{lim}}{i_{ss}} - 1\right) + i_{ss}\, R_{cell} \qquad [13]$$

where ΔV is the applied cell voltage, $\Delta E_{1/2}$ is the difference in half-wave potentials between the $A/A^{-\cdot}$ and $D/D^{+\cdot}$ reactions, and i_{ss}^{lim} is the limiting steady-state current which obtains when the parent concentrations at the electrode surface are essentially zero. The ECL intensity, I, is proportional to the flux of $A^{-\cdot}$ and $D^{+\cdot}$ at the middle of the cavity and hence is proportional to the current

$$I = \phi_{ECL}\, i_{ss}/n\mathbf{F} \qquad [14]$$

just as in RRDE experiments (19).

The behavior of thin-layer ECL cells was tested using the rubrene in benzonitrile and $Ru(bip)_3^{2+}$ in ACN systems. Satisfactory lifetimes could only be obtained when no supporting electrolyte (TBAP) was added to the cell solution. For the $Ru(bip)_3^{2+}$ system this cation and the ClO_4^- counterion served as electrolyte. For the rubrene system, small amounts of impurities, perhaps introduced in the drying stages, probably served as electrolyte until the concentration of electrogenerated ions built up to aid in the conduction. The results, shown in Fig. 9 and 10, fit the predicted behavior quite well. The lack of proportionality of I and i_{ss} at low i_{ss} values shown in Fig. 10, is reminiscent of the "foot" observed in I *vs.* disk current in RRDE ECL studies (19), ascribed there to reaction of low levels of impurities with the excited states.

The rise time in a thin-layer ECL cell depends upon the time required for $A^{-\cdot}$ and $D^{+\cdot}$ to diffuse together after the current flow commences and for the current to decay to its limiting value. To a first approximation then, light emission should commence at $t_s = l^2/16D$, (or for $l = 100$ and 20 μm, t_s is of the order of one and 0.04 sec, respectively). A more sluggish response suggests the occurrence of some slow chemical step or quenching of the excited state species. In the absence of complications the intensity should then level off at the value given by Eq. [14] (Fig. 11). In all cases we have observed a decay in signal level with time, probably indicative of the processes which limit the lifetime of the large cells but which are greatly accelerated because of the small cell volume. We should note that while half-lifetimes of about 10 min can be obtained in cells that contain no added TBAP, those that contain the usual 0.1M levels of TBAP have considerably

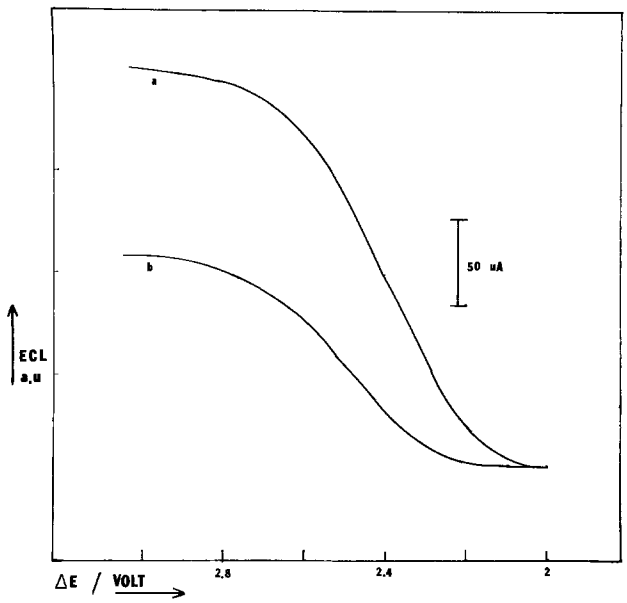

Fig 9. Thin-layer ECL for 4 mM rubrene/BZN for 50μ spacing and scan rate of 2 mV/sec. (a) Current *vs.* applied voltage; (b) light intensity *vs.* applied voltage.

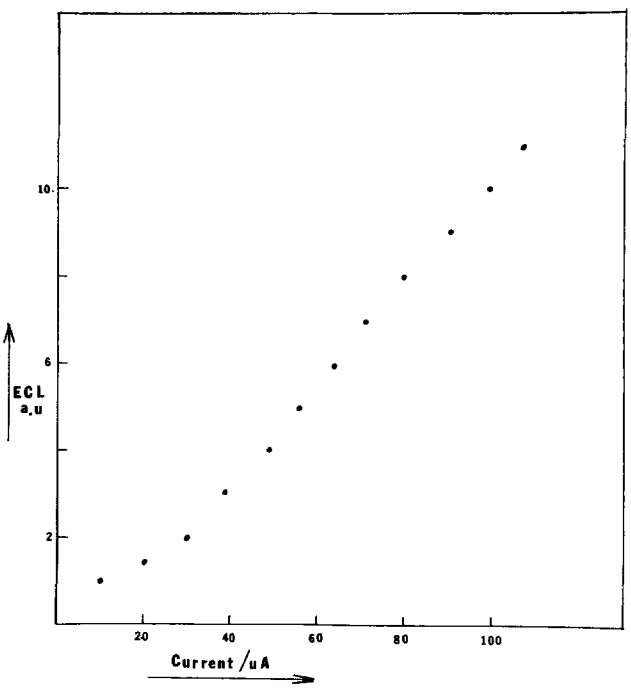

Fig. 10. Light intensity *vs.* applied d.c. in thin-layer ECL (conditions as in Fig. 9).

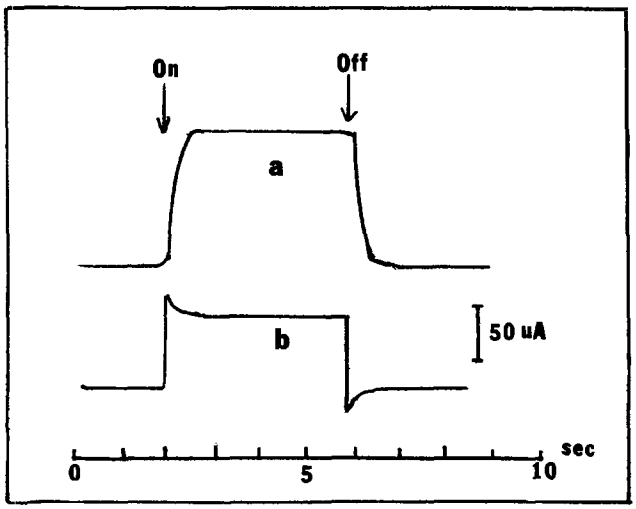

Fig. 11. Transients in thin-layer ECL. (a) Light intensity; (b) current cell. Spacing, 30μ (other conditions as in Fig. 9).

shorter lifetimes (maximum of about 3 min), suggesting that the supporting electrolyte may be an important source of impurities or quencher progenitors in ECL systems.

The thin-layer cell can also be operated in the pulsed cyclic mode. For pulse lengths small with respect to the time to diffuse half the cell thickness, the previous two-electrode treatments apply. For pulse lengths of the order of t_s, when the electrode polarity is reversed a sharp light spike is observed, because of the new annihilation reactions occurring near the electrodes; the light then decays until the mid-cell reaction becomes important and the light increases again toward its steady-state value (Fig. 12). In both the d.c. and pulsed mode thin-layer ECL cells will be useful in studying decay mechanisms in ECL cells and in accelerated life testing.

The small interelectrode spacing of the thin layer ECL cell makes possible the use of solvent systems which would be too resistive for conventional electrochemical cells. For example a solution of 10^5 ohm-cm specific resistance will only produce a 50 mV iR drop

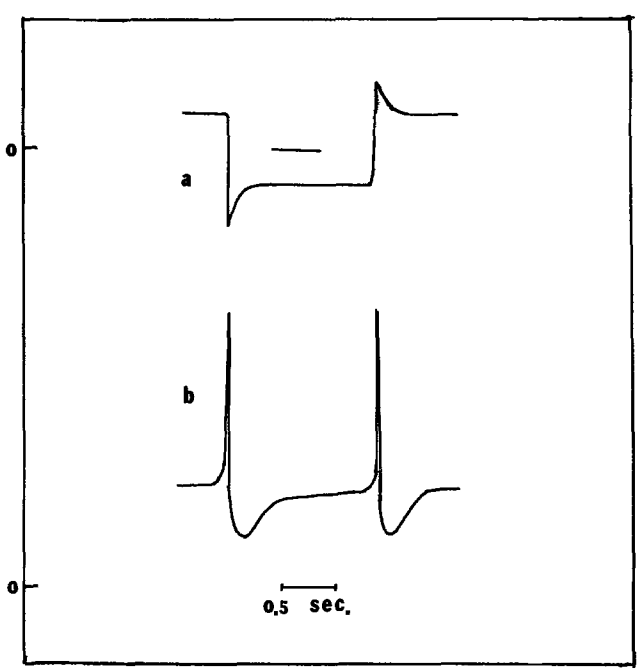

Fig. 12. Effect of reversal of electrode polarity in thin-layer cell. (a) Current; (b) light intensity (cell and solution as in Fig. 11).

for $l = 20$ μm and a current density of 250 μA/cm^2. In the presence of low electrolyte concentrations very high fields can be produced inside the cell by using external high voltage sources. These would lead to appreciable migration of the electrogenerated species, *i.e.*, in effect the $D^{+\cdot}$ and $A^{-\cdot}$ would be "fired" at one another by the large field gradient. The study of ECL and electrochemical reactions under these conditions is potentially of interest and is currently under study.

Steady-state efficiency of ECL cells.—The measurement and kinds of efficiency in ECL have been discussed (14, 19, 33). What is of interest in ECL devices is $\bar{\phi}_{coul}^{ss}$, the number of photons emitted per number of faradaic electrons passed, per pulse, after sufficient repetitive cycles that steady-state electrochemical behavior is observed

$$\bar{\phi}_{coul}^{ss} = \frac{\int_0^{t_f} I dt_N}{\int_0^{t_f} i dt_N} \qquad [15]$$

The maximum value of this parameter, which applies when $\phi_{ECL} = 1$, *i.e.*, when every radical ion encounter produces an emitted photon, depends on the mode of electrical excitation and cell geometry. This can be estimated by digital simulation (13, 14, 20) of repetitive pulses with the appropriate boundary conditions. The efficiencies quoted here are based on simulations in which only a single species (*e.g.*, species A) is the parent of both radical ions ($A^{-\cdot}$ and $A^{+\cdot}$) and all species have equal diffusion coefficients. It is assumed that the radical annihilation reaction is diffusion controlled and leads directly to an emitting species which emits with unit efficiency (luminescence quantum yield of one). The simulation employed 2000 simulation time units (L) per pulse.

For the pulse potentiostatic (three-electrode) mode, assuming that only the working electrode emits, the following values of $\bar{\phi}_{coul}$, obtained by counting the total number of annihilations per pulse and dividing by the total electric charge required in that pulse, were obtained beginning with pulse 1 (production of $A^{+\cdot}$: pulse 1, 0; 2, 0.549; 3, 0.462; 4, 0.507; 5, 0.484; 6, 0.494; 7, 0.491; 8, 0.489. Thus the limiting value of $\bar{\phi}_{coul} \cong 0.49$. For example, during a cathodic pulse, N, 49% of the current produces $A^{-\cdot}$ which reacts with the $A^{+\cdot}$ produced during the previous pulse (N − 1) and the remainder produces excess $A^{-\cdot}$ which will react with $A^{+\cdot}$ in the pulse N + 1. Only about 2% of the current is consumed by direct reduction of $A^{+\cdot}$ (in the two-electron reaction to form $A^{-\cdot}$) at the electrode and very little of the $A^{-\cdot}$ produced in this pulse will eventually diffuse into bulk solution. Steady state is attained after about 7 or 8 pulses, and at steady state the concentration profiles of the electrogenerated species ($A^{-\cdot}$ in pulse N) and the reacting previously generated species ($A^{+\cdot}$ in pluse N − 1) are essentially the same from pulse to pulse except for a small diminishing tail of the species first produced ($A^{+\cdot}$ in the example) spreading out into the bulk solution. The value $\bar{\phi}_{coul}^{ss} = 0.49$ implies that under ideal conditions, the coulombic efficiency approaches the maximum possible value for pulsed ECL efficiency (0.50) and that few faradaic electrons are lost in the process. For two-electrode cells in the voltage pulsed mode, for case (a) (large auxiliary electrode), the maximum value of $\bar{\phi}_{coul}^{ss}$ is the same as in the potentiostatic case. For case (b) (electrodes of equal size), both electrodes will emit, so the over-all cell efficiency can

approach a maximum value of 98%. In the constant current mode, because of the greater extent of nonradiative radical ion loss by direct electrode reaction, the maximum efficiency per electrode is only 30% (or 60% for emission at both electrodes). The thin-layer d-c cell will show a maximum efficiency of 100%, since every radical ion produced should ultimately annihilate in the middle of the cell. The practical efficiencies of cells will depend on the actual value of ϕ_{ECL} (for the most efficient systems, this lies in the range of 0.01 to 0.1), the magnitude of the nonfaradaic current and the cell resistance.

Acknowledgment

The support of this research by the U.S. Army Research Office-Durham is gratefully acknowledged.

Manuscript submitted Oct. 29, 1974; revised manuscript received Dec. 24, 1974.

Any discussion of this paper will appear in a Discussion Section to be published in the December 1975 JOURNAL. All discussions for the December 1975 Discussion Section should be submitted by Aug. 1, 1975.

Publication costs of this article were partially assisted by The University of Texas at Austin.

REFERENCES

1. T. Kuwana, in "Electroanalytical Chemistry," A. J. Bard, Editor, Vol. 1, Chap. 3, Marcel Dekker, New York (1966).
2. A. J. Bard, K. S. V. Santhanam, S. A. Cruser, and L. R. Faulkner, in "Fluorescence," G. G. Guilbault, Editor, Chap. 14, Marcel Dekker, New York (1967).
3. A. Zweig, *Advan. Photochem.*, **6**, 425 (1968).
4. E. A. Chandross, *Trans. N. Y. Acad. Sci. Ser. 2*, **31**, 571 (1969).
5. D. M. Hercules, *Accounts Chem. Res.*, **2**, 301 (1969).
6. D. M. Hercules, in "Physical Methods of Organic Chemistry," A. Weissberger and B. Rossiter, Editors, 4th Ed., Part II, Academic Press, New York (1971).
7. A. J. Bard and L. R. Faulkner, in "Creation and Detection of the Excited State," W. R. Ware, Editor, Vol. 3, Marcel Dekker, New York (In press).
8. J. T. Bowman and A. J. Bard, Unpublished results; see J. T. Bowman, Ph.D. Dissertation, The University of Texas at Austin (1971).
9. C. P. Keszthelyi and A. J. Bard, Unpublished results; see C. P. Keszthelyi, Ph.D. Dissertation, The University of Texas at Austin (1973).
10. R. M. Measures, *Appl. Optics*, **13**, 1121 (1974).
11. C. P. Keszthelyi and A. J. Bard, *This Journal*, **120**, 241 (1973).
12. M. M. Nicholson, *ibid.*, **119**, 461 (1972).
13. S. A. Cruser and A. J. Bard, *J. Am. Chem. Soc.*, **91**, 267 (1969).
14. R. Bezman and L. R. Faulkner, *ibid.*, **94**, 3699 (1972).
15. Y. Murata and H. J. Shine, *J. Org. Chem.*, **34**, 3368 (1969).
16. L. S. Marcoux, *J. Am. Chem. Soc.*, **93**, 537 (1971).
17. V. D. Parker, *J. Electroanal. Chem.*, **36**, App. 8, (1972).
18. R. Dietz, A. E. J. Forno, B. E. Larcombe, and M. E. Peover, *J. Chem. Soc., (B)*, (**1970**), 141.
19. J. T. Maloy and A. J. Bard, *J. Am. Chem. Soc.*, **93**, 5968 (1971).
20. S. W. Feldberg, *ibid.*, **88**, 390 (1966).
21. N. E. Tokel and A. J. Bard, *ibid.*, **94**, 2862 (1962).
22. N. E. Tokel-Takvoryan, R. E. Hemingway, and A. J. Bard, *ibid.*, **95**, 6582 (1973).
23. J. A. Seckel, T. M. Huret, and J. T. Maloy, Abstract No. 63, 24th Pittsburgh Conference on Analytical Chemistry and Applied Spectroscopy, March 5-9, 1973.
24. H. J. S. Sand, *Phil Mag.*, **1**, 45 (1901).
25. T. Berzins and P. Delahay, *J. Am. Chem. Soc.*, **75**, 4205 (1953).
26. H. Gerischer and M. Krause, *Z. Physik Chem. (N.F.)*, **10**, 264 (1957); **14**, 184 (1958).
27. A. T. Hubbard and F. C. Anson, "Electroanalytical Chemistry," A. J. Bard, Editor, p. 129, Marcel Dekker, New York (1971).
28. A. T. Hubbard, *CRC Crit. Rev. Anal. Chem.*, L. Meites, Editor, p. 201, Chemical Rubber Co., Cleveland, Ohio (1973).
29. C. N. Reilley, *Rev. Pure Appl. Chem.*, **18**, 137 (1968).
30. P. T. Kissinger, (Michigan State Univ.), Private communication.
31. J. S. Dunnett and M. Voinev, (Battelle-Geneva), Private communication.
32. J. Murphy, (Westinghouse Corp.), Private communication.
33. A. J. Bard, C. P. Keszthelyi, H. Tachikawa, and N. E. Tokel, "Chemiluminescence and Bioluminescence," M. J. Cormier, D. M. Hercules, and J. Lee, Editors, Plenum Press, New York (1973).

Technical Notes

Penetration of Hydrogen into Aluminum on Exposure to Water

Henry Leidheiser, Jr.* and Narayan Das

Center for Surface and Coatings Research, Lehigh University, Bethlehem, Pennsylvania 18015

Data in the literature indicate that hydrogen has limited solubility in aluminum (1, 2) equilibrated with gaseous hydrogen. For example, the solubility of hydrogen in pure aluminum at 300°C is reported to be of the order of 0.001 ml/100g. The solubility increases to approximately 0.04 ml/100g at 660°C. Our immediate interest was to determine the amount of hydrogen that penetrates into aluminum as a consequence of exposure of the metal to water.

* Electrochemical Society Active Member.
Key words: hydrogen, aluminum, aqueous corrosion.

Aluminum samples were in the form of flat plates, approximately 12 × 1 × 0.1 cm. The composition was 99.994% aluminum, 0.003% copper, 0.002% iron, and 0.001% silicon. The samples were metallographically polished, washed with ethanol and acetone, dried in vacuum for 6 hr, and annealed at 600°C for 4 hr at a pressure of 10^{-6} Torr. The samples were then cooled in vacuum and exposed to liquid water at 60°-100°C for varying periods of time. After exposure to water, the corrosion product was removed by heating in a mixture of 2% CrO_3 and 5% H_3PO_4 at 95°C for 60 min.